Chapter 3

Zinc Oxide and Magnesium Doped Zinc Oxide Decorated Nanocomposites of Reduced Graphene Oxide as Friction and Wear Modifiers

Chapter 3

Graphene being a two-dimensional structure of sp^2 carbon atoms in a honeycomb lattice has acquired importance owing to its remarkable mechanical and optical properties, physical strength, thermal conductivity, and resistivity to permit entry of gases or liquids [Geim (2009), Zhu et al. (2010), Ferrari et al. (2015)]. In addition to these properties, graphene has proved to be an apt material as an antiwear and antifriction agent [Berman et al. (2014), Ota et al. (2015), Peng et al. (2015), Restuccia et al. (2016), Eswaraiah et al. (2011)]. On account of strong π-π interactions and van der Waals attractive force between the graphene sheets, graphene is amazingly easy to agglomerate, especially in lubricating oil, resulting in weak dispersibility, which limits its application in the field of industrial lubrication. Hybrid nanomaterials, if engineered carefully, may result in the enhancement of desirable properties [Zhu et al. (2011)]. The composites of graphene with metal oxide are fairly known in the literature, but those with doped metal oxides are rarely studied for their lubricating properties. Hybrid nanomaterials, if engineered carefully, may result in the enhancement of desirable properties [Zhu et al. (2011)]. The composites of graphene with metal oxide are fairly known in the literature, but those with doped metal oxides are rarely studied for their lubricating properties [Bai et al. (2014), Zhou et al. (2015)].

Zinc oxide has an open hexagonal type of crystal structure, which facilitates the formation of defects through doping [Kalyani et al. (2016)]. These defects result in the formation of slip systems and lower shear strength. Excellent results were obtained when zinc oxide was doped with magnesium (SDS-stabilized $Zn_{0.88}Mg_{0.12}O$). This prompted us to combine the advantages of the layered structure of reduced graphene oxide (rGO) and highly

efficient magnesium doped zinc oxide nanoparticles (ZMO) in the form of the nanocomposite, ZMO-rGO and compare its tribo-characteristics with those of the nanocomposite of pure ZnO, ZnO-rGO. In the present investigation, reduced graphene oxide (rGO) was prepared by the method reported in the literature [Umrao et al. (2015)]. Pure zinc oxide (ZnO), and magnesium doped zinc oxide nanoparticles, $Zn_{0.88}Mg_{0.12}O$ (ZMO), were prepared by the auto-combustion method [Kalyani et al. (2016)]. The well-characterized nanoparticles were used to prepare nanocomposites, ZnO-rGO, and ZMO-rGO. Morphology and microstructures of nanoparticles and their nanocomposites have been studied by SEM/HR-SEM, EDX, TEM/HR-TEM, XRD, FTIR, Raman, UV/visible, and XPS techniques.

Evaluation of lubricating properties of reduced graphene oxide nanosheets (rGO), nanoparticles (ZnO and ZMO), and their composites ZnO-rGO, ZMO-rGO, has been carried out by four- ball tribotester. The observed data prop up synergy between nanoparticles and rGO. Since doping of ZnO with magnesium already has yielded good results, ZMO-rGO composite, as expected, behaves superior to ZnO-rGO. Surface studies of the wear scar by SEM and AFM and chemical analysis by XPS support these results.

3.1. Materials and Methods

3.1.1. Chemicals

Analytical Reagent grade chemicals were used throughout the present investigation as such without following any purification process. Extra pure Zn $(NO_3)_2.6H_2O$, Mg $(NO_3)_2.6H_2O$,

ethanol, and anhydrous citric acid were procured from Merck. Besides these, graphite flakes (1-2 mm, NGS Naturgraphit GmbH), Potassium Permanganate ($KMnO_4$, ≥99.0%, Fluka), Ethanol (CH_3CH_2OH, ≥98% Sigma-Aldrich) were also acquired. The other general chemicals, such as ammonia solution, H_2SO_4, H_3PO_4, H_2O_2, $N_2H_4.H_2O$, etc., were procured from Merck, India.

3.1.2. Synthesis of Additives

3.1.2.1. Preparation of GO and rGO

The graphene oxide (GO) and microwave-assisted reduced graphene oxide (rGO) have been synthesized by the same procedure as reported earlier [Umrao et al. (2015)].

3.1.2.2. Preparation of ZnO and Magnesium-Doped ZnO (ZMO) Nanoparticles

Synthesis of ZnO and magnesium doped ZnO (ZMO, $Zn_{0.88}Mg_{0.12}O$) nanoparticles was accomplished by the auto-combustion method [Kalyani et al. (2016)]. For ZnO, $Zn(NO_3)_2.6H_2O$ (14.27 g) and citric acid (6.26 g) were mixed in 25 ml of double-distilled water. The aqueous solution was kept on a hot plate at approximately 200 ^oC with uninterrupted stirring till the gel formed burns ultimately. The burning of gel results in the formation of blackish ash. As prepared, ash was calcined at 600 ^oC in the air for 4h to give ZnO nanoparticles. The magnesium doped zinc oxide nanoparticles (ZMO) were prepared similarly, adding magnesium nitrate hexahydrate (1.63g) in the required amount before evaporation of an aqueous solution on a hot plate.

3.1.2.3. Preparation of Composites of ZnO/ZMO and rGO

Suspensions of ZnO nanoparticles (700 mg/100 mL of ethanol) and rGO (1 mg/mL) were prepared by about one-hour sonication at ~50 °C. Both suspensions were mixed with perpetual stirring. Sonication of the mixed suspensions at 70 °C yielded black colored material. It was filtered, dried at 50 °C, and kept in a microwave oven for 3 min at 700 W. Finally, a black colored composite of ZnO nanoparticles with nanosheets of reduced graphene oxide (ZnO-rGO) was obtained.

A similar procedure was adopted for the preparation of nanocomposite of ZMO and rGO.

3.2. Sample Preparation

The admixtures of paraffin oil with different additives, zinc oxide/magnesium doped zinc oxide nanoparticles, and their corresponding composites with reduced graphene oxide were prepared in varying concentrations 0.0000, 0.0625, 0.1250, 0.1875, and 0.2500 % (w/v) by sustained stirring at 45-55 °C for 2h followed by sonication for 1h at room temperature. The tribological tests were performed at an optimized concentration, i.e., 0.125% w/v of rGO, ZnO, ZMO, ZnO-rGO, ZMO-rGO, in the base oil.

3.3. Results and Discussion

3.3.1. Characterization of Additives

As-synthesized zinc oxide and magnesium doped zinc oxide nanoparticles and their corresponding composites with reduced graphene oxide were characterized by SEM/HR-SEM, TEM/HR-TEM, XRD, FT-IR, Raman, UV/visible, and XPS techniques.

The HR-SEM images of nanosheets of rGO, nanoparticles of ZMO (ZnO doped with Mg, $Zn_{0.88}Mg_{0.12}O$, and composite ZMO-rGO are displayed in **Fig. 3.1a**, **1b**, and **1c**, respectively. The SEM image of rGO shown in Figure1a distinctly establishes a layered structure. **Fig. 3.1c** perspicuously reveals ZMO nanoparticles (27 nm) garnishing graphene sheets. The chemical composition of the ZMO-rGO nanocomposite was obtained from its EDX spectrum, Figure1c. Signals due to zinc, magnesium, and oxygen, along with carbon, are clearly visible in the spectrum, indicating the formation of the proposed nanocomposite. The atomic weight % data, tabulated in the inset of **Fig. 3.1c**, support the formation of the ZMO-rGO nanocomposite.

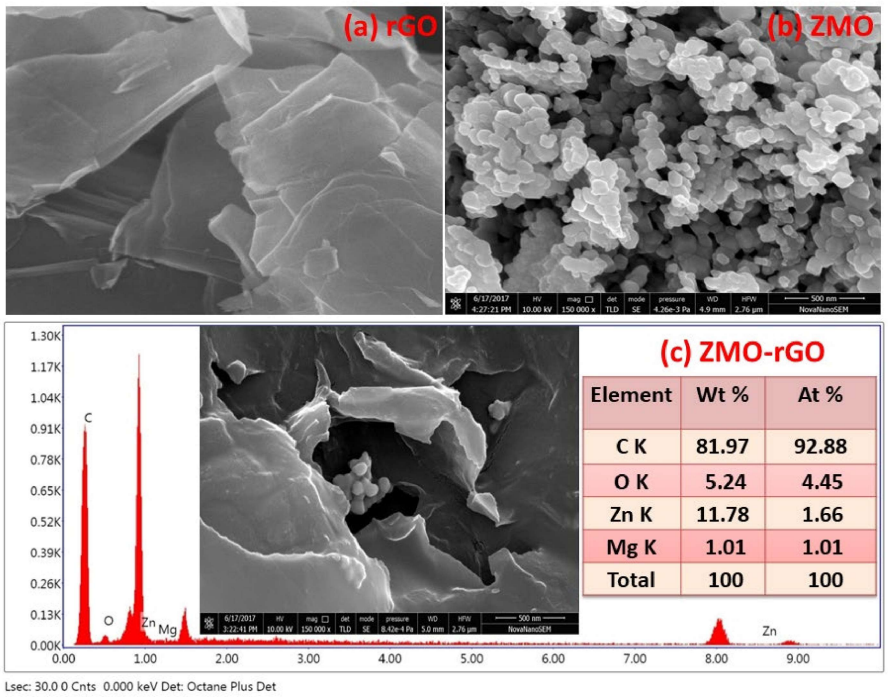

Fig. 3.1. HR-SEM images of (a) rGO, (b) ZMO, and (c) ZMO-rGO with the EDX spectrum

For a proper understanding of morphology, TEM images have been taken and are illustrated in **Fig. 3.2**, rGO (a), ZnO (b), ZMO (c), and ZMO-rGO (d), respectively. HR-TEM images of rGO and ZMO-rGO are also shown in **Fig. 3.2(a_1)** and **2(d_1),** respectively. The hexagonal shape of nanoparticles ZnO and ZMO is apparent in the TEM images, **Fig. 3.2b,** and **2c**. The size of the nanoparticle appears to be in the range of 25-30 nm. **Fig. 3.2(a_1)** exhibits a layered structure of graphene. TEM and HR-TEM images of ZMO-rGO, **Fig. 3.2d,** and **2d_1** clearly show nanoparticles with reduced size (15-20 nm) anchored on the graphene surface.

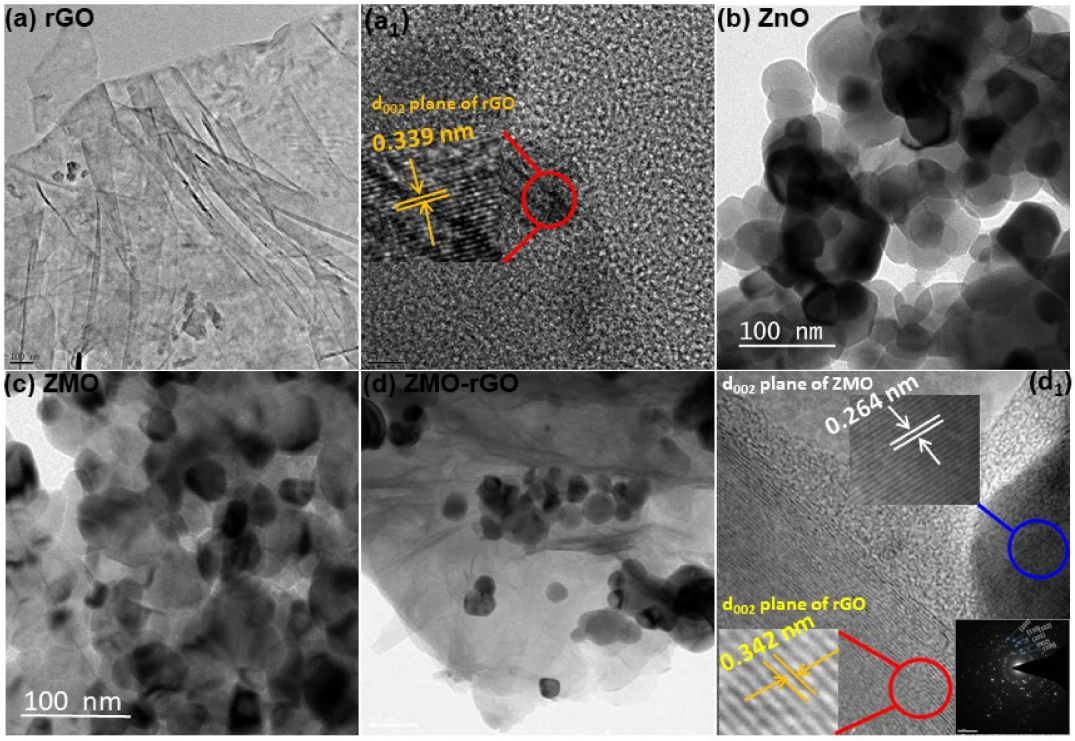

Fig. 3.2. TEM images of (a) rGO, (b) ZnO, (c) ZMO, (d) ZMO-rGO and HR-TEM images of (a_1) rGO and (d_1) ZMO-rGO. The inset in (d_1) provides the SAED pattern of ZMO-rGO.

Fig. 3.3a illustrates X-ray diffraction (XRD) patterns of rGO, ZnO, ZMO, ZnO- rGO, and ZMO-rGO. The reported characteristic peak of GO at about 11° due to (001) reflection is conspicuously absent in diffraction patterns of rGO or its composites, indicating the reduction of GO to rGO. A small peak around 26.5° in the diffraction pattern of rGO is attributed to (002) reflection with an interlayer spacing of 0.35 nm [Jaiswal et al. (2016)]. It is apparent from the diffraction patterns that ZMO and the composites still retain the hexagonal wurtzite structure of ZnO (JCPDS No. 36-1451) [Kalyani et al. (2016)]. The addition of magnesium has not produced any additional peak showing the formation of a single phase. However, the intensity of the peaks has fairly reduced, particularly in the composite. Using the Debye-Scherrer formula, the size of nanoparticles has been calculated as 30 and 27 nm for ZnO and ZMO, respectively.

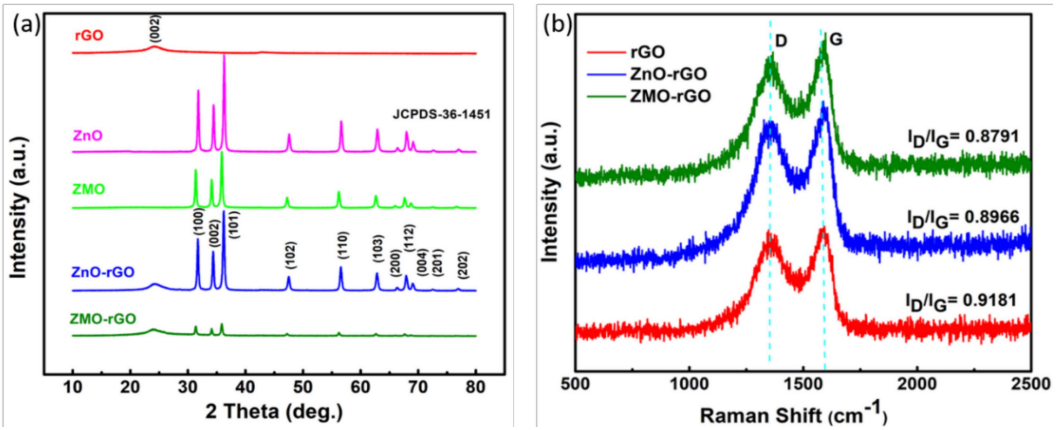

Fig. 3.3. (a) XRD patterns of as-prepared rGO, ZnO, ZMO nanoparticles, and their nanocomposites, ZnO-rGO and ZMO-rGO (b) Raman spectra of rGO, ZnO-rGO, and ZMO-rGO.

Typical Raman spectra of rGO and its composites, using 532 nm laser excitations, are displayed in **Fig. 3.3b.** The strong peaks near 1360 and 1582 cm^{-1} are ascribed to D and G bands of graphene, respectively [Jaiswal et al. (2016), Li et al. (2011), Zhan et al. (2012)]. The G band has undergone a positive shift in the composites appearing at 1590 and 1597 cm^{-1} in ZnO-rGO and ZMO-rGO, respectively [Li et al. (2011), Zhan et al. (2012)]. The D band (appearing due to breathing mode of A1g symmetry) corresponds to sp^3/sp^2 hybridized defects, while the G band (doubly degenerate phonon mode of E2g symmetry) corresponds to vibration in the sp^2 bonded carbon atoms. The ratio of the intensity of these bands, I_D/I_G, reflects density defects or disorders in the structure [Li et al. (2011)]. Its value has sufficiently decreased in the composites compared to rGO, showing that the defects of rGO have been reconciled by ZnO/ZMO or the area of crystalline rGO has increased.

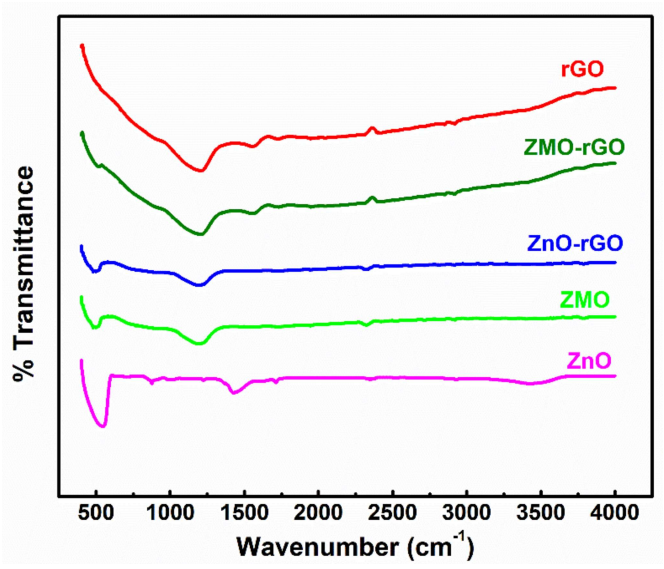

Fig. 3.4. FT-IR spectra of rGO, ZnO, ZMO, ZnO-rGO, and ZMO-rGO nano additives

The characteristic peaks of GO due to oxygen-containing groups were found to be almost absent in the FT-IR spectra of rGO and its composites, indicating a reduction of GO, **Fig. 3.4**. A characteristic peak for the Zn-O stretching mode has been observed in the region 480-520 cm^{-1} in the spectra of zinc oxide and the composites [Li et al. (2011), Wang et al. (2014)]. However, the intensity of the band in the composites is comparatively much reduced.

Fig. 3.5 exhibits UV-visible diffuse reflectance spectra (DRS) of all the additives recorded in the range of 200-900 nm. It is clearly visible from the spectra that the absorption peak observed at 375 nm has undergone a blue shift in ZMO, indicating a widening of the bandgap. A comparison of spectra of ZMO-rGO and ZnO-rGO reveals a similar kind of blue shift in this band. The spectral evidence supports the formation of ZMO and its nanohybrid with rGO [Wang et al. (2014)].

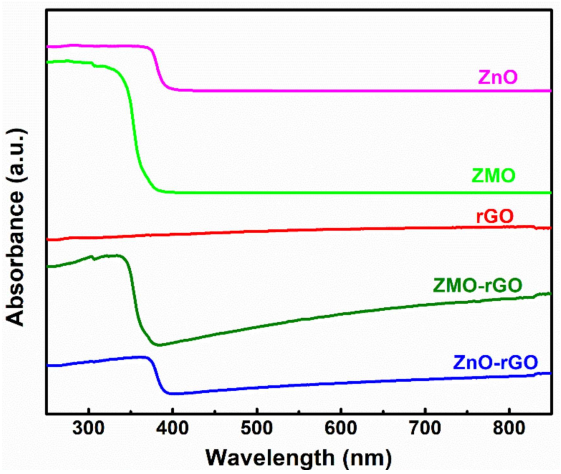

Fig. 3.5. UV-visible diffuse reflectance spectra of rGO, ZnO, ZMO, ZnO-rGO, and ZMO-rGO nano additives

The XPS measurements have been used to study the chemical structure of composite ZnO-rGO. XPS survey of the nanohybrid reveals the presence of C, O, and Zn having atomic % 72.74, 19.71, 7.55, respectively.

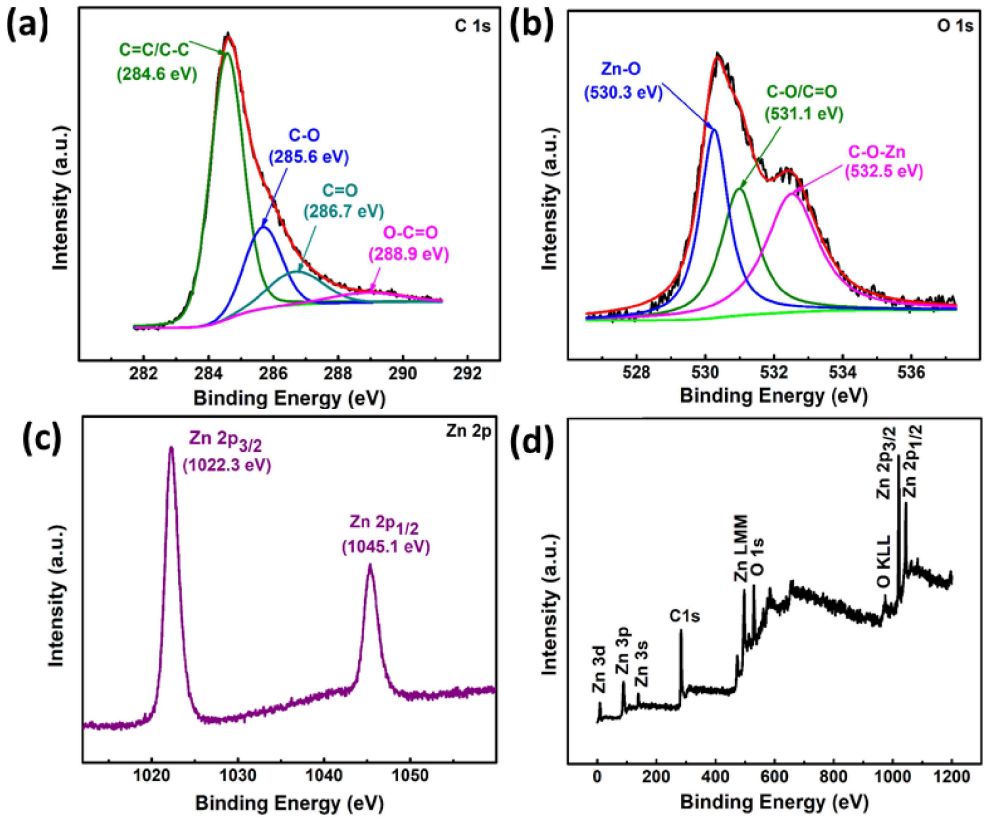

Fig. 3.6. Deconvoluted XPS spectra of ZnO-rGO nanomaterial: (a) C 1s core-level spectra, (b) O 1s core-level spectra, (c) Zn 2p core-level spectra and (d) XPS survey spectra.

Fig. 3.6 shows its core level spectra deconvoluted with best-fitting parameters based on peak fit software. **Fig. 3.6a** clearly depicts core level spectra of C 1s deconvoluted into 4 peaks with binding energies 284.6, 285.6, 286.7, and 288.9 eV, which correspond to C=C, C-O, C=O, and O-C=O bonds respectively [Li et al. (2011), Zhan et al. (2012)]. **Fig. 3.6b** exhibits

core level spectra of O 1s deconvoluted into three peaks at 530.3 for Zn-O, 531.1 for C=O/C-O, and 532.5 eV for C-O-Zn [Jaiswal et al. (2016)]. **Fig. 3.6c** shows Zn 2p core-level spectrum characterized by peaks due to Zn $2p_{3/2}$ and Zn $2p_{1/2}$ with binding energies 1022.3 and 1045.1 eV, respectively [Li et al. (2011)].

3.3.2. Dispersion Stability of Nanofluids in Base Oil

Dispersion stability of the additives rGO, ZnO, ZMO, nanohybrids ZnO-rGO, and ZMO-rGO in base oil was evaluated with the help of electronic spectra. At first, the optimized concentration of the additives, 0.125% w/v, was dispersed in paraffin oil using an ultrasonicator for 1h. The dispersions thus prepared were further 10 times diluted, and their absorbance was recorded in the range of 200-800 nm at different intervals starting from zero time up to 48 hours.

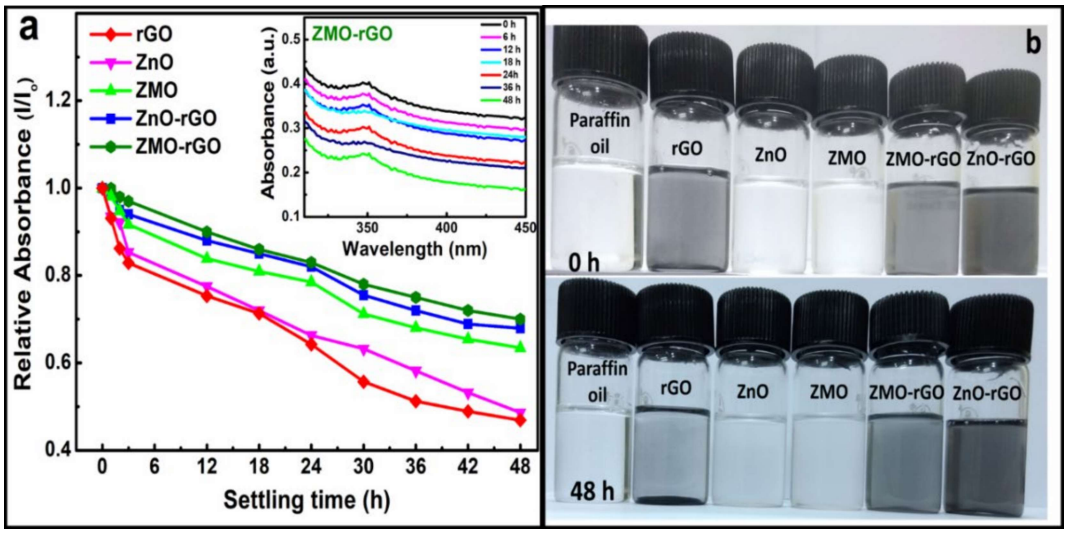

Fig 3.7. (a) Dispersion stabilities of base oil containing rGO, ZnO, ZMO, ZnO-rGO, and ZMO-rGO studied by UV-vis spectrophotometry (b) Optical photographs of different nano additives dispersed in base oil at different settling times.

The graph plotted between relative absorbance and settling time for each of the additives is displayed in **Fig 3.7a**. It is clearly evident from the figure that relative absorbance decreases with time in every case, but the extent of decrease is widely different for the studied additives throughout 48 hours and follows the order given below-

rGO > ZnO > ZMO > ZnO-rGO > ZMO-rGO

The above order reflects that the dispersion of ZMO-rGO possesses maximum stability, but other additives are also sufficiently stable as relative absorbance has gone down upto nearly 0.5. For the sake of brevity, the absorbance of only ZMO-rGO dispersion at different intervals beginning from zero h to 48 h has been shown in the inset. It is apparent that the nanohybrid absorbs at 354 nm, and absorbance decreases from around 0.4 to 0.2 within 48 hours. The photographs of base oil and its dispersions with the additives at zero time and after 48 hours are shown in **Fig 3.7b.**

3.3.3. Tribological Properties

Tribological properties are concentration-dependent; therefore, before starting the tribological experiments, optimization of the concentration of the additives must be performed. **Fig 3.8** depicts mean wear scar diameter (MWD) as a function of additive concentration at a load of 392N for 60 min test duration in base lube paraffin oil. It is evident from the figure that the values of MWD are significantly reduced in the presence of the blends of additives in paraffin oil at all the concentrations compared to paraffin oil alone. Thus, all additives are capable of boosting the antiwear properties of base oil at each concentration. In

the beginning, at 0.0625% w/v concentration of rGO, the MWD has dropped sufficiently from that of blank paraffin oil, 0.733 mm. Further decrease in its value is observed when nanoparticles ZnO and the ZMO are subsequently used. In the presence of composite ZnO-rGO again, it decreases, and the maximum decrease is visible for ZMO-rGO admixture. When concentration is increased to 0.125% w/v, the lowering of MWD follows the same order for different additive blends. At the next higher concentration, 0.1875 % w/v, there is a slight increase in MWD in the case of rGO and nanoparticles ZnO or ZMO, but the composites show a much larger increase. The optimum concentration for all the experiments, therefore, has been kept as 0.125 % w/v. This is a noteworthy point that at the next higher concentration, 0.25% w/v small decrease in MWD is observed in all cases except ZMO, where a drastic decrease is identified. Maximum reduction in MWD is noted in the presence of ZMO-rGO at all the tested concentrations before 0.25% w/v.

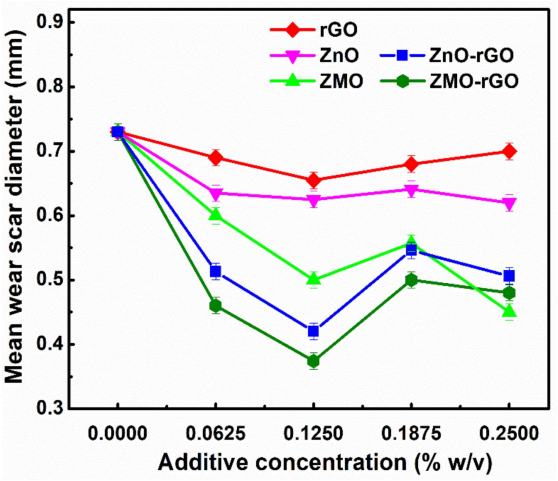

Fig. 3.8. Variation of mean wear scar diameter for the paraffin oil as a function of additive concentration at 392 N applied load for 60 min duration

The potentiality of nanoparticles, ZnO/ZMO, and their nanohybrids with rGO as antiwear additives was adjudged by ASTM D4172 test in paraffin oil at 392 N load for 60 min test duration. The test results are represented in **Fig.3.9.** as a bar diagram envisaging a comparative picture of mean wear scar diameter (MWD) and the average coefficient of friction (COF) values together.

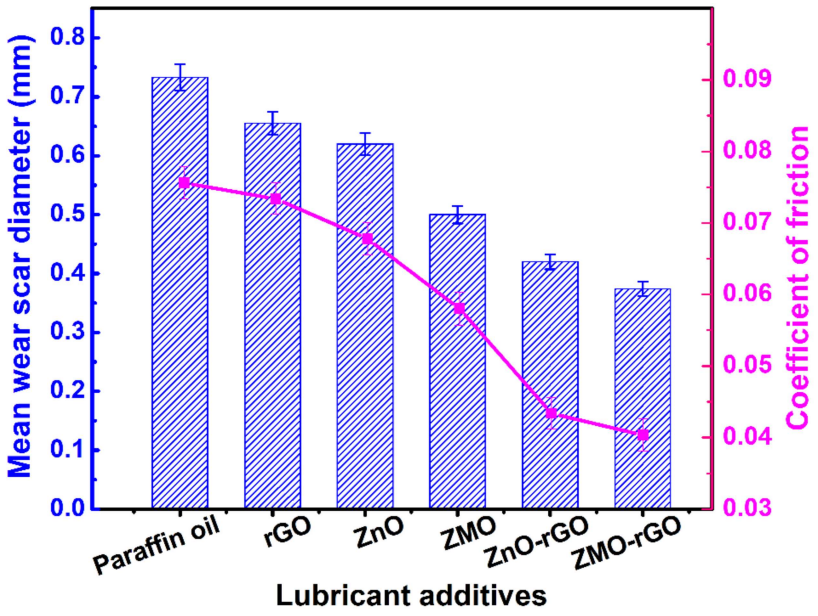

Fig. 3.9. Variation in the mean wear scar diameter and coefficient of friction in the presence of nano additives in paraffin oil: load, 392 N; sliding speed, 1200 rpm; temperature, 75 °C; test duration, 60 min; concentration of additives, 0.125% w/v.

It is perceptible from the figure that the value of MWD 0.733 mm for blank oil has gradually decreased through its blends (showing % reduction) with rGO (11%), ZnO (15%), ZMO (32%), ZnO-rGO (43%) and finally reached to the lowest value 0.374 mm (49%) in case of ZMO-rGO. This drop-in MWD is indicative of the relative antiwear performance of different

additives. The average COF value in base lube, 0.0756, shows a similar trend in % reduction in the presence of different additives rGO (3%), ZnO (10%), ZMO (23%), ZnO-rGO (42%), and ZMO-rGO (47%). Thus, in the presence of additives, tribochemical film of low shear strength is formed *in situ* under operating conditions, which resists the metal-metal contact and safeguards the matting surfaces from friction and wear. It is important to mention here that composites with a greater reduction in MWD and COF values act as excellent wear and friction modifiers owing to the reinforcement of rGO by nanoparticles ZnO/ZMO. In fact, nanoparticles as nano-bearing and rGO with lamellar structure have collectively improved the efficiency of composites. The better efficiency of the composite of ZMO over that of ZnO may be interpreted in terms of higher thermal conductivity of ZMO than ZnO, which has resulted in a lowering of local temperature at asperities on the metal surface [Kalyani et al. (2016)]. Consequently, the dissipation of heat has provided better lubrication.

Fig. 3.10 depicts how the friction coefficient of steel surface varies with time at 392 N load in base oil alone or its blends. No doubt, the friction coefficient values are always higher for the base lube than its blends throughout the test. In the presence of rGO as an additive, the COF values are reduced considerably, but with the passage of time, a slight increase in the values is also observed. The slight increase may be due to little agglomeration of rGO with an increase in sliding time. Agglomeration of rGO perturbs its continuous access over the surface. When the mating surfaces are supplemented with admixtures containing nanoparticles, COF values are further reduced and stabilized. Needless to mention, that

reduction in COF is more for ZMO. The nanoparticles behaving as nano-bearings at the interacting surfaces account for a drastic reduction in COF data. COF values are severely reduced and stabilized in the presence of composites, particularly ZMO-rGO. Thus, the doping of magnesium to ZnO has enhanced the friction-reducing characteristics of the composite. Since the stability of COF values is directly related to the life of machine parts, it is a very important property of an additive. Furthermore, COF values are usually a little higher in the beginning due to the absence of tribofilm. Later with increasing sliding time, tribofilm is formed, and accordingly, COF is lowered.

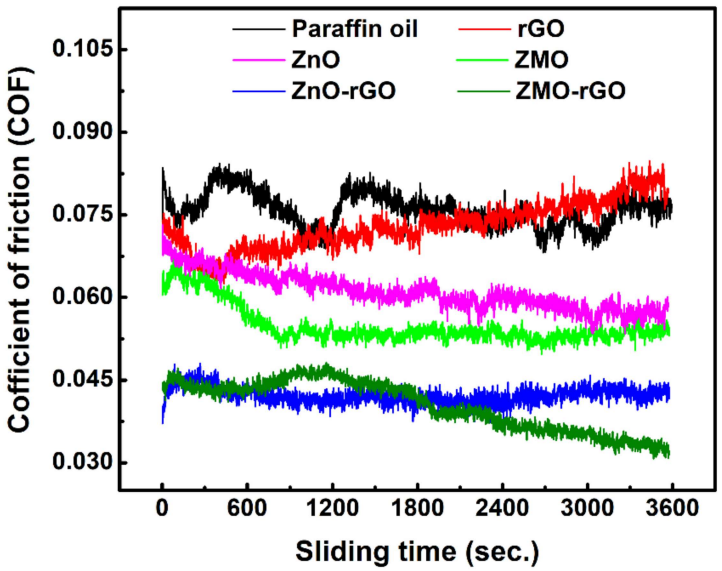

Fig. 3.10. Variation of the coefficient of friction with sliding time in the presence of different nano additives (0.125% w/v) in paraffin oil: load, 392 N; speed, 1200 rpm; temperature, 75 ^{o}C; test duration, 60 min.

The wear rate has been determined by conducting the test for different periods of sliding time 0.25, 0.50, 0.75, 1, 1.25, and 1.5 h under the load of 392 N in base oil with or without additives. From the observed MWD values for different sliding periods, mean wear volume (MWV) has been calculated since it is a more appropriate parameter for calculating the wear rate [Kalyani et al. (2016)]. **Fig. 3.11** shows a plot between MWV values and sliding time from 0 to 1.5 h. A linear regression model has been fitted to obtain the wear rate. The running-in and steady-state periods are considered to lie between 0-0.75 h and 0.75-1.25 h, respectively.

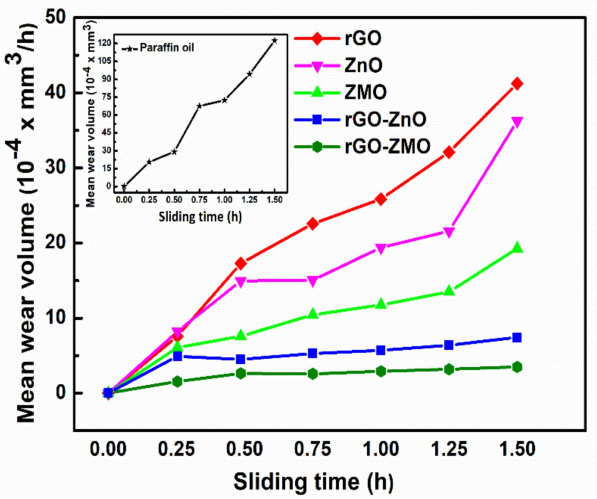

Fig. 3.11. Variation of mean wear volume with time for paraffin oil containing (0.125% w/v) nano additives at 392N applied load

Accordingly, running-in and steady-state wear rates have been determined as per **Fig. 3.12** and **3.13**, respectively, and the corresponding data are collected in **Table 1**. The high values of running-in and steady-state wear rates in the presence of base oil alone get appreciably lowered in the presence of additives. The magnitude of lowering appears to be

in accordance with the antiwear properties of the additives discussed above. Moreover, the steady-state wear rate, as expected, is lower than the corresponding running- in wear rate. The low value of a steady-state wear rate enhances the life expectancy of the machine components. Thus, maximum lowering in running-in, as well as steady-state wear rates, is discernible when the interacting tribo pairs are supplemented with admixture containing ZMO-rGO, the most favored candidate for tribological application in industry.

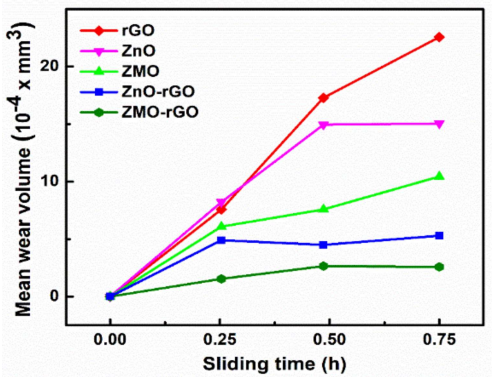

Fig. 3.12. Determination of running-in wear rate by varying mean wear volume with time (h) for paraffin oil containing (0.125% w/v) nano additives at 392N applied load

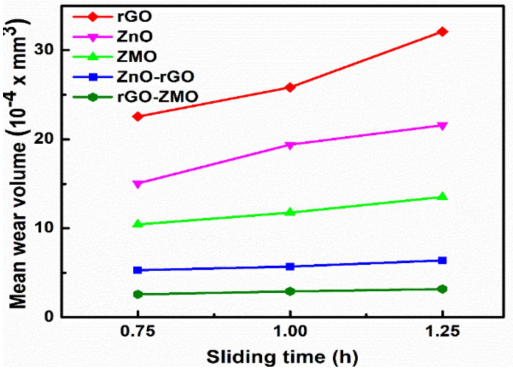

Fig. 3.13. Determination of steady-state wear rate by varying mean wear volume with time (h) for paraffin oil containing (0.125% w/v) nano additives at 392N applied load

Table 3.1. Wear-rate for paraffin oil in the presence and absence of nano additives for 60 min test duration at 392 N applied load

S.N.	Lubricants	Wear rate (10^{-4} × mm^3/h)	
		Running-in	Steady-state
1	Paraffin oil	84.48	53.32
2	rGO	31.07	18.78
3	ZnO	20.77	9.46
4	ZMO	13.24	7.53
5	ZnO-rGO	6.24	2.40
6	ZMO-rGO	3.55	0.75

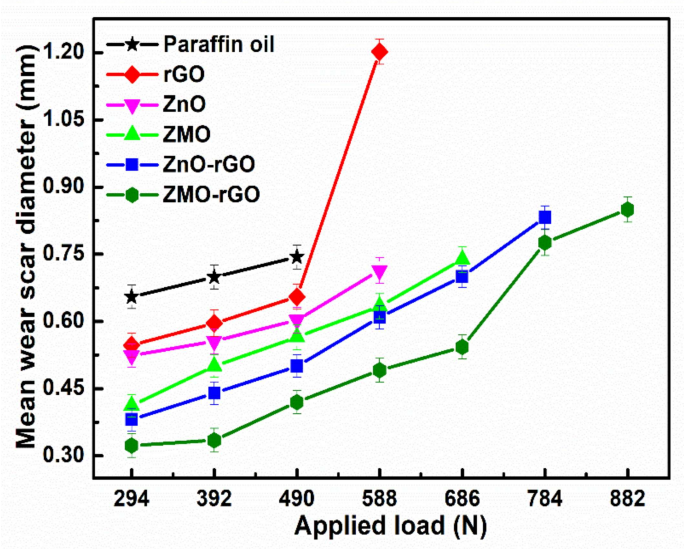

Fig. 3.14. Variation of mean wear scar diameter with applied load for paraffin oil containing 0.125% w/v of different nano additives for 30 min test duration

Variation of MWD as a function of applied load in the absence and presence of different additives in base lube for 30 min sliding time is illustrated in **Fig. 3.14**.

It is apparent from the figure that with an increase of applied load, MWD increases as well. The increase of load creates higher pressure on the contact surfaces, which in turn decreases film thickness and facilitates metal-metal contact through asperities; as a result, MWD is increased. The values of MWD are observed to be much higher in the presence of plain base oil without additives at each tested load as compared to the surface lubricated with admixtures. The order of reduction of MWD in the presence of various additives at each load is in conformity with the order evolved from the antiwear test ASTM D4172. The MWD is very large at the beginning at 294 N load, in base oil alone but in the presence of the blends, it is considerably reduced. At the next higher load, 392 N, a similar pattern of MWD is observed for different additives. The base oil fails completely after 490 N to sustain the load. In the case of the admixture containing rGO, an abrupt increase in MWD is observed at 490 N load. It cannot be used, therefore, beyond 490N load. On further increasing the load, it is vividly seen that in the presence of blends with nanoparticles, the in situ formed tribofilm successfully bears the load upto 588 N and 686 N for ZnO and ZMO, respectively. The load-bearing ability is further improved upto 784 N and 882 N when nanohybrids ZnO-rGO and ZMO-rGO are tested as additives. The maximum load-bearing ability is, therefore, observed with nanohybrid ZMO-rGO.

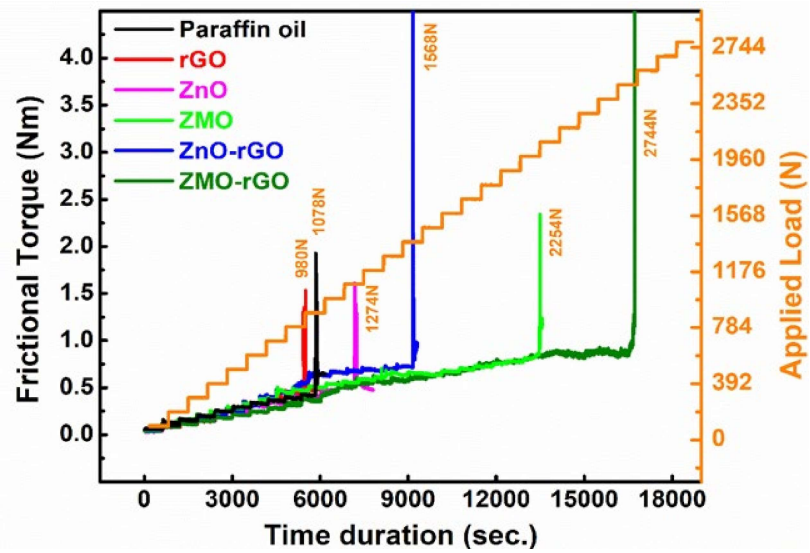

Fig. 3.15. Variation of frictional torque as a function of stepwise loading and time for different nano additives: sliding speed, 600 rpm; temperature, 75°C; concentration of additives, 0.125% w/v.

For the load ramp test (ASTM D5183), at first, a test has been performed for the optimized concentration of all the additives under the conditions; 392 N load, 600 rpm, temperature 75°C, and 60 min time duration, so that the running-in period is over. The steady-state coefficient of friction test was conducted by adding subsequently 98 N load after every 10 min. The test results are displayed in **Fig. 3.15**.

The value of frictional torque appears to be higher in the absence of additives than in their presence. With an increase in load and time together, the difference in frictional torque values between the base lube and its admixtures has widened. In the presence of admixtures, frictional torque values are comparatively much lower but more stable than the base oil at

each applied load. In the case of plain paraffin oil enormous increase of frictional torque at 1078 N results in seizure between the interacting surfaces. At seizure load, the breakdown of tribofilm disturbs the steady-state, and lubricant fails. Surprisingly, the seizure load for admixture containing rGO is very low (980 N), even below base oil. The behavior of rGO may be ascribed to its poor adhering capability. The presence of additives other than rGO, of course, increases the seizure load ZnO (1274 N), ZnO-rGO (1568 N), ZMO (2254 N), and ZMO-rGO (2744 N). Thus, reinforcement of rGO by ZnO/ZMO is evident from the above data. Besides this, the supremacy of the additive ZMO-rGO over ZnO-rGO and the nanoparticles is again quite clear from this test, indicating that doping of ZnO with Mg is beneficial in enhancing the lubrication property of the composite.

3.3.4. Morphological Studies of Worn Surface

Use has been made of surface techniques, AFM, and SEM for morphological studies of the wear scar on the steel ball surface lubricated with paraffin oil and its blends containing different additives (0.125% w/v) under ASTM D4172 conditions. The SEM micrographs for base oil and its blends are displayed in **Fig. 3.16**. In the presence of plain paraffin oil, SEM images reveal large furrows due to awful scuffing. The surface is undoubtedly improved in the presence of all the blends. The order of improvement in surface corresponds very well to the antiwear properties of the studied additives. Needless to mention that phenomenal smoothness of the surface is observed in the case of nanohybrids, particularly ZMO-rGO. The value of MWD (shown in the inset of each micrograph) 0.733 mm for base oil has

decreased substantially in the presence of all the additives ZnO (0.620), ZMO (0.500), ZnO-rGO (0.420), and finally, ZMO-rGO (0.374 mm). Gradation of MWD can be directly correlated with the smoothness of the surface.

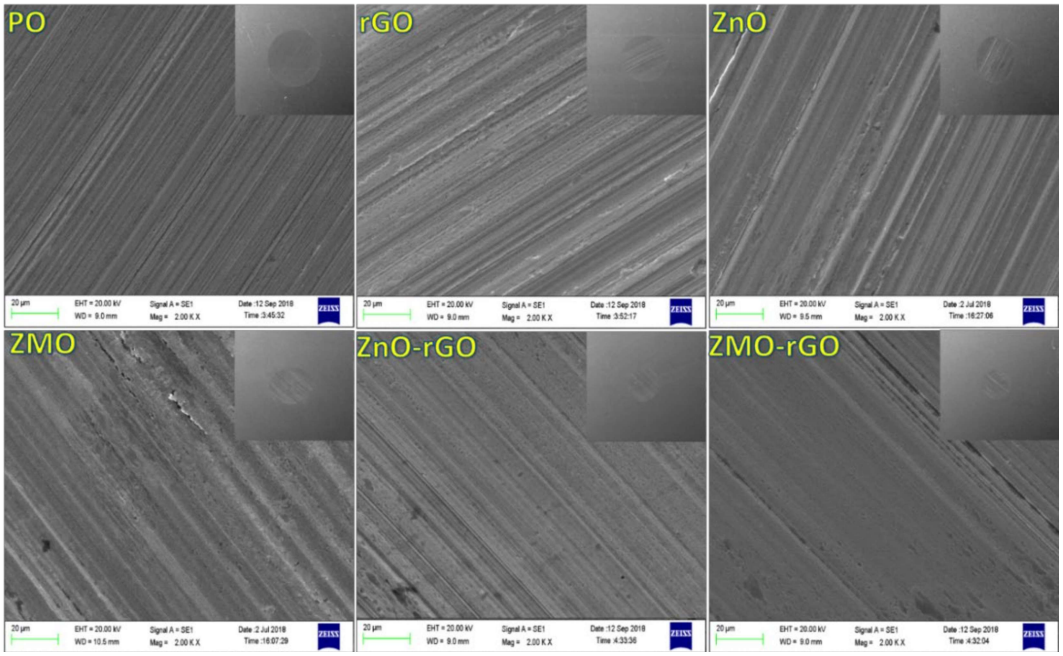

Fig. 3.16. SEM micrographs (inset giving a full view of wear scar at 100X, wear scar surface at 2.00 KX magnification) of the worn steel surface lubricated with paraffin oil in the presence and absence of different nano additives (0.125% w/v) for 60 min test duration at 392 N applied load.

Contact mode AFM was used to study morphological features of steel ball surfaces lubricated with paraffin oil with or without additives after the ASTM D4172 test. **Fig. 3.17** exhibits 2D and 3D AFM images of worn steel surfaces along with surface roughness values, line roughness (Rq), and area roughness (Sq). As apparent from the figure, there is a drastic

reduction in the values of Rq and Sq from blank paraffin oil to ZMO-rGO through rGO, ZnO, ZMO, and ZnO-rGO. Thus, AFM results support very well the observation based on SEM studies.

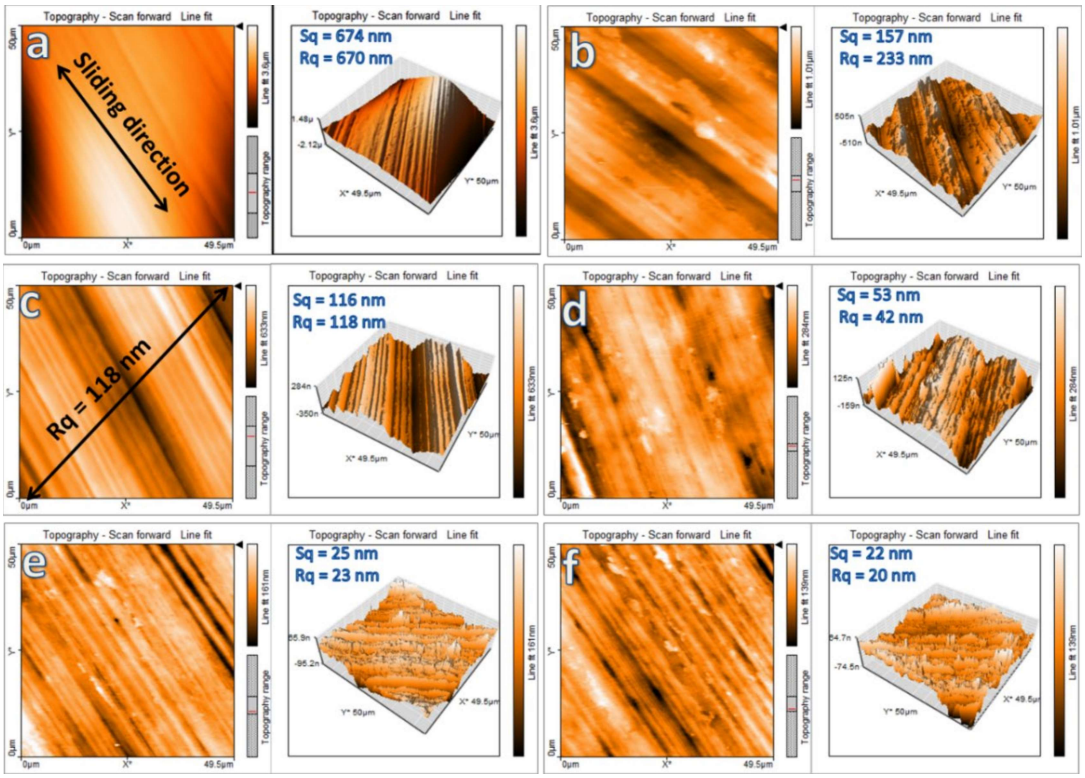

Fig. 3.17. *2D* and *3D* AFM images of the worn steel surface lubricated with different additives (0.125% w/v) in paraffin oil for 60 min test duration at 392 N applied load: (a) Paraffin oil, (b) rGO, (c) ZnO, (d) ZMO, (e) ZnO-rGO and (f) ZMO-rGO.

3.3.5. Characterization of Tribofilm and Tribo-Chemistry

EDX spectra of the worn surface lubricated with blends of optimized concentration of nanohybrids in base oil at 392 N applied load shown in **Fig. 3.18** provide the elemental

composition of the tribofilm. In addition to peaks in base oil (**Fig. 3.18c**), **Fig. 3.18a** exhibits an extra peak due to zinc, while extra peaks due to zinc and magnesium both are evident in **Fig. 3.18b**. The presence of these peaks supports the tribo-sinterization mechanism for lubrication.

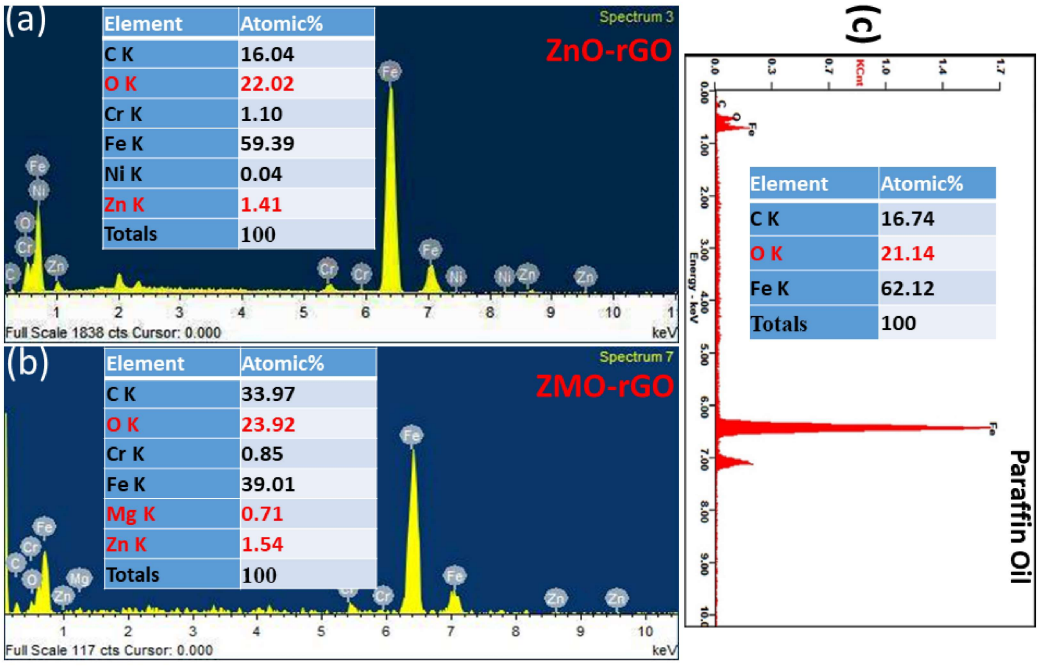

Fig. 3.18. EDX spectra of worn surface lubricated with (0.125% w/v) (a) ZnO-rGO (b) ZMO-rGO nano additives and (c) Blank Paraffin oil at 392N applied load

The XPS spectra of the steel surface lubricated with an admixture of paraffin oil with ZMO-rGO were recorded after ASTM D 4172 test to find out the chemical composition of the in situ formed tribofilm, **Fig. 3.19**. The spectra were deconvoluted with XPS peak software after subtracting the Shirley background. The figure exhibits XPS spectra (curve

fitted) of C 1s, O 1s, Mg 1s, Zn 2p, and Fe 2p of the worn surface in the presence of ZMO-rGO additive in the base oil.

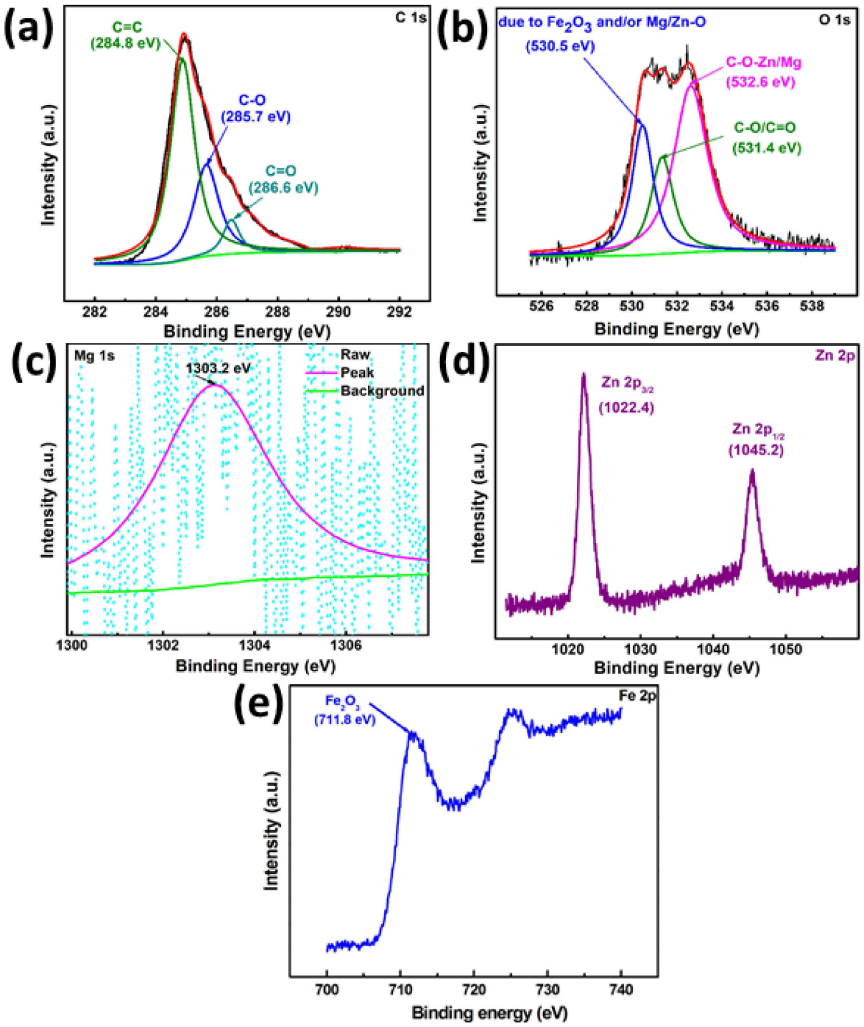

Fig. 3.19. Deconvoluted XPS spectra of the tribofilm formed on the steel surface lubricated with ZMO-rGO nanocomposite under ASTM D4172 test conditions: (a) C 1s spectra, (b) O 1s spectra, (c) Mg 1s spectra, (d) Zn 2p spectra, and (e) Fe 2p spectra.

Fig. 3.19a. exhibits core level spectra of C 1s deconvoluted into four peaks with binding energies 284.8, 285.7, and 286.6 eV corresponding to C=C, C-O, and C=O bonds, respectively [Jaiswal et al. (2016)]. The position of these peaks is approximately similar to that of the XPS spectra of ZnO-rGO.

Fig. 3.19b displays core level spectra of O 1s deconvoluted into 3 peaks, the first one at 530.5 eV for Fe2O3, ZnO, and/or MgO, the second peak at 531.4 eV for C-O/C=O, and the third peak at 532.6 eV for C-O-Zn/Mg [Jaiswal et al. (2016)]. **Fig. 3.19c.** shows a peak with binding energy 1303.2 eV ascribed to Mg 1s [Aksoy et al. (2012)]. The peaks due to Zn 2p3/2 and Zn 2p1/2 with binding energies 1022.4 and 1045.2 eV, respectively, are observed in the XPS spectra of ZMO-rGO after ASTM D4172 test in **Fig. 3.19d** [Li et al. (2011)]. The absence of any appreciable shift in these peaks from XPS spectra of ZnO-rGO taken before the ASTM D4172 test reveals that ZnO nanoparticles are tribo-sintered on the interacting surface. Under the test conditions, the iron of the steel surface is definitely oxidized to Fe_2O_3; therefore, the signal for Fe 2p is observed with binding energy 711.8 eV, as apparent in **Fig. 3.19e** [Jaiswal et al. (2016)].

3.3.6. Proposed Mechanism of Lubrication

As discussed above, all the nano additives cling to the proximal surfaces and form a tribofilm in situ under experimental test conditions that actually bears the load. However, the incredibly high performance of the studied composites/nanohybrids emphasizes the synergistic interaction between their constituent nanoparticles and rGO. It may be convincingly stated that drastic reinforcement of rGO has been achieved through

nanoparticles. Undoubtedly, the nanoparticles anchored between rGO nanosheets have substantially prevented the restacking of rGO nanosheets. At the same time, nanosheets of rGO have helped in alleviating the agglomeration of nanoparticles. These nanoparticles act as nano bearings between rGO layers and interacting surfaces as well, resulting in enhanced feasibility of sliding motion and finally increasing lubrication. Tribo-sinteriztion of the nanoparticles on the tribo pairs also adds to increased lubrication behavior as small pits on the damaged surface are repaired. Replacement of ZnO by ZMO in the composite has further enhanced its tribological behavior terribly. As reported earlier, doping of magnesium in ZnO increases thermal conductivity that, in turn, reduces the temperature at the asperity, and lubricating properties are enhanced. Besides this, the hexagonal open type of crystal structure of zinc oxide has facilitated the formation of defects through doping, resulting in the formation of slip systems, which have lowered the shear strength. The outstanding tribological performance of the blend containing the nanocomposite ZMO-rGO is attributed to the *in situ* formed tribofilm composed of mainly oxides, Fe_2O_3, ZnO, and MgO on the lubricated matting surface.

3.4. Conclusions

The zinc oxide (ZnO) and 12% magnesium doped zinc oxide, ZMO ($Zn_{0.88}Mg_{0.12}O$) nanoparticles have been synthesized by the auto-combustion method. Nanocomposites of as-prepared nanoparticles with microwave synthesized reduced graphene oxide nanosheets, ZnO-rGO and ZMO-rGO, have been prepared and characterized by advanced techniques

such as Raman, FT-IR, and electronic spectroscopy, SEM/HR-SEM with EDX, TEM/HR-TEM, powder XRD, and XPS. Dispersion stability of the blends of nanohybrids ascertained by electronic spectroscopy reveals that these are almost stable up to 48 hours. Evaluation of the tribological activity of the synthesized nanoparticles/nanosheets and nanocomposites in paraffin base oil has been performed invoking tribological parameters, mean wear scar diameter (MWD), coefficient of friction (COF), load-carrying capacity, and wear rates obtained from ASTM D4172, and ASTM D5183 tests using four-ball lubricant tester at the optimized concentration, 0.125% w/v. The friction/wear-reducing efficiency and load-carrying capacity of different additives in paraffin oil followed the order given below:

ZMO-rGO > ZnO-rGO > ZMO > ZnO > rGO > paraffin oil

Explicitly high activity of nanocomposites depicts a strong synergy between nanoparticles and rGO. The surface morphology studies by SEM and surface roughness data obtained from AFM micrographs of the wear scar also support the above order. The best efficiency shown by the composite ZMO-rGO may be directly related to adequate reinforcement of rGO by zinc and magnesium oxide as the presence of these oxides is witnessed in EDX analysis of the worn surface. The vital role played by these oxides in lubrication is further established from XPS studies of the tribofilm. Thus, having magnesium doped ZnO in the composite has yielded fruitful results. Based on the above, the candidacy of the composites, specifically ZMO-rGO, as potential wear and friction modifiers appears to be well justified under boundary lubricating conditions.